Applications of vector calculus in modeling source-sink dynamics among metapopulations

Author(s): William M. Webb
Source: BIOS, 83(3):97-103. 2012.
Published By: Beta Beta Beta Biological Society
DOI: http://dx.doi.org/10.1893/0005-3155-83.3.97
URL: http://www.bioone.org/doi/full/10.1893/0005-3155-83.3.97

Preliminary Report

Applications of vector calculus in modeling source-sink dynamics among metapopulations

William M. Webb

Millsaps College, Jackson, MS 39210

Abstract. Operating under several assumptions regarding density-dependant dispersal, a novel way of visualizing the source-sink dynamics of metapopulations is introduced in which vector calculus operators were applied to approximated surface functions. First, occurrence data were used to create a population density matrix for a fictional *Genus species*, which was modeled as a 3-dimensional scatter plot. Next, the data were fitted to an approximated function corresponding to the data's 3-dimensional surface, permitting the data to be treated as a scalar field. This scalar field was then subjected to the gradient and divergence operators to produce a mathematical model of *G. species* migration and source-sink dynamics, respectively.

Introduction

Classic metapopulation theory holds that a large metapopulation, or "population of populations," may be comprised of distinct, local subpopulations within spatially separate patches of habitat (Levins, 1969). Within these metapopulations, some subpopulations may inhabit areas that experience local mortality rates in excess of local reproductive rates, thereby creating a "sink" habitat. If this habitat is to remain populated, new individuals must replace them via immigration from more favorable and thus, more productive, "source" habitats (Pulliam, 1988). In this way, subpopulations within a metapopulation are connected by migration, despite exhibiting their own extinction and colonization dynamics. Classically, these source-sink dynamics have been treated as occurring under "spatially heterogeneous, but temporally constant, conditions" (Johnson, 2004), and it is under this assumption that the proposed model is most useful.

While compared sampling at different points in time can produce a quantitative model for population change among arbitrarily sized patches of habitat, the instantaneous role of a habitat as a source or a sink can only be inferred qualitatively, and never as a precise, continuous gradient across infinitely many or indefinitely small patches (Hanski, 1991). The utility of the proposed model lies in its ability to take a set of population density data over spatially heterogeneous conditions and transform it into a scalar field where the expected approximate population at any given point in space is returned as an output and for which traditional vector calculus operators can be employed.

One way that a prediction about a patch's tendency to behave as a source or a sink could be made is if the population experienced density-dependent dispersal, but empirical support for this assumption is mixed (Amarasekare,

Correspondence to: webbwm@millsaps.edu
Key words: ecology; ecological modeling

Bios 83(3) 97–103, 2012

2004). While some consider population density to be unrepresentative of habitat productivity (Van Horne, 1983) and independent of dispersive tendency, many studies have shown that at least some species do in fact conform to a density-dependant model in which individuals are most likely to move from areas of high population density to areas of low population density (see Fonseca and Hart, 1996, for insects; Veit and Lewis, 1996, for birds; and Aars and Ims, 2000, for mammals).

In this light, the proposed model assumes density-dependant dispersal where individuals are most likely to move from areas of high population density to areas of low population density, and where more productive patch-habitats will exhibit greater source behavior as a consequence of increasing population density. It is under these two assumptions that the proposed model is useful and under these circumstances that it ought to be employed.

Materials and Methods

First, occurrence data were artificially created for a fictional *Genus species*. The metapopulation of *G. species* was imagined to inhabit a similarly fictional island of area 100 km^2 which, as a perfect square, was subdivided into 100 patches of habitat into a 10 $\times$ 10 km grid. Population sampling was imagined to have been performed under controlled conditions at the midpoint of each square km. The data collected, displayed as number of individuals collected per square km, revealed a metapopulation comprised of three major subpopulations with largely uninhabited areas in between (Table 1). In this way, suitable, productive habitat patches could be said to exist within a matrix of unsuitable space.

In order to fit the occurrence data to a 3-dimensional, differentiable function that returned its data points at the appropriate coordinates, the data were converted into a 3-variable t-chart (where z is a function of x and y, and z represents population at a given set of coordinates) and entered into the ZunZun.com 3-D Function Finder interface, in accordance with its required data entry format (Table 2). Coefficients to acceptable surface functions were fitted to 319 different non-linear template equations by their lowest sum of squared absolute error (SSQ), the standard approach to 3-dimensional data fitting in regression analysis (Christopolous, 2000; Lancaster et al., 1986). The interface was instructed to find up to 25 coefficients per function (the maximum number) in order to ensure maximum smoothness of the final surface.

Next, the returned functions were ranked by their sum of squared absolute error, as well as by their coefficients of determination and their simplicity (e.g., with polynomials taking precedence over rational or logarithmic expressions). The first-ranked of these equations was a polynomial and had the highest rank by both lowest sum of squared absolute error and by coefficient of determination. (It is shown in its entirety under Results and depicted as a surface and a contour map in Figures 1 and 2, respectively.) This equation has been approximated below in an abridged version (with only 6 coefficients, each rounded to three decimal places) to illustrate the operations that were performed upon it:

$$z(x,y) = 6.868 - 9.530y + 3.597y^2 - 0.526y^3 + 0.026y^4 - 13.478x \ldots$$

With this function, the approximate population density of *G. species* could be determined around any set of coordinates, essentially permitting the data to be treated as a scalar field. As a scalar field, the function was differentiable by the vector calculus gradient operator (expressed as *grad*, or the "nabla" symbol ∇), where for a given function z:

$$grad(z) = \nabla z(x,y) = \left(\frac{\partial z}{\partial x}, \frac{\partial z}{\partial y}\right) = \frac{\partial z}{\partial x}\hat{\imath} + \frac{\partial z}{\partial y}\hat{\jmath}$$

$\ldots$ producing a vector field. This new function, now a vector field, could be denoted $\vec{z}$, and was itself differentiable by the divergence operator (expressed as *div*, or the "nabla" symbol and the dot product $\nabla\cdot$), where for a given function $\vec{z} = U\hat{\imath} + V\hat{\jmath}$:

$$div(\vec{z}) = \nabla \cdot \vec{z}(x,y) = \frac{\partial U}{\partial x} + \frac{\partial V}{\partial y}$$

Taking the gradient of the scalar field population

Table 1. Sample occurrence data for the fictional *G. species* was generated such that its metapopulation on a fictional 100 × 100 km island contained three major subpopulations with less suitable habitats in between.

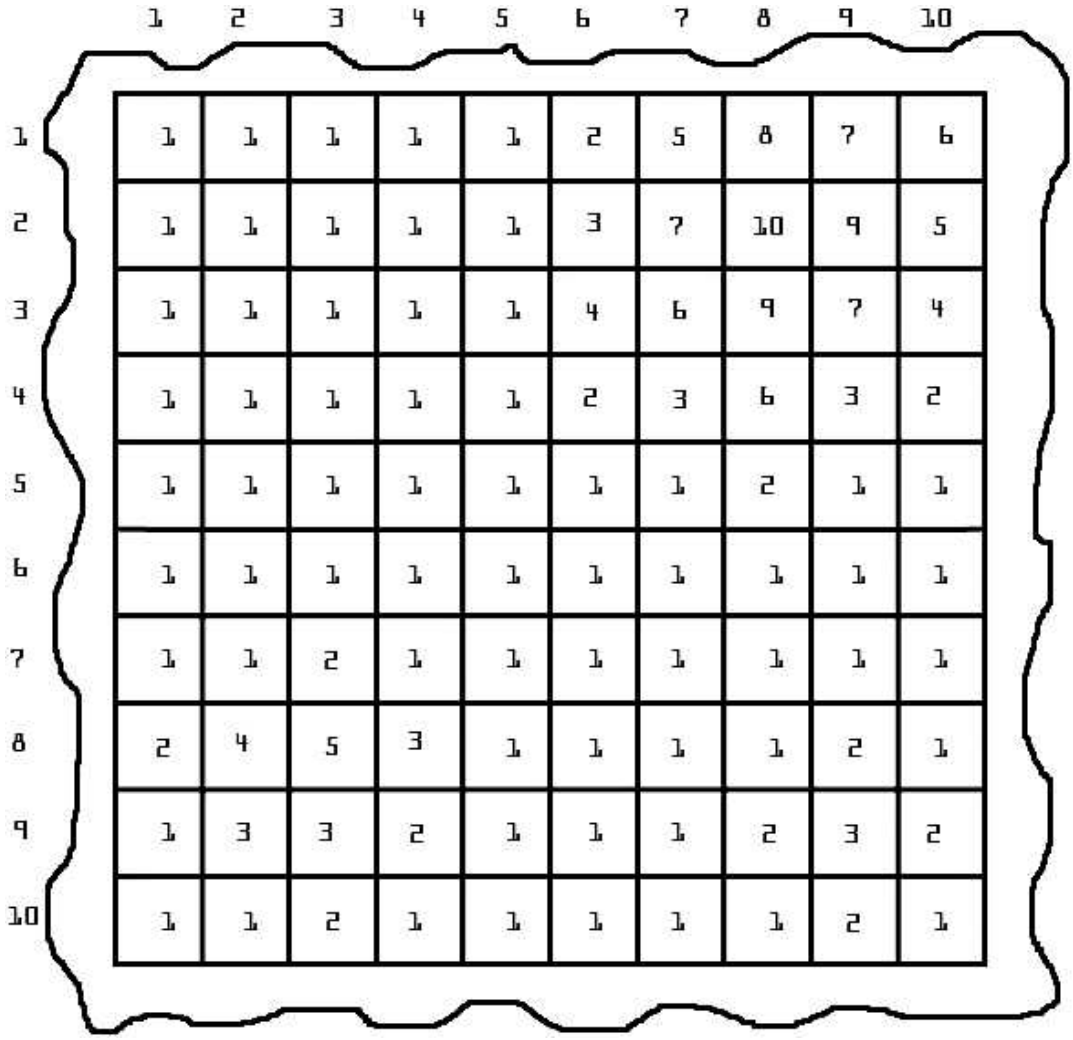

	1	2	3	4	5	6	7	8	9	10
1	1	1	1	1	1	2	5	8	7	6
2	1	1	1	1	1	3	7	10	9	5
3	1	1	1	1	1	4	6	9	7	4
4	1	1	1	1	1	2	3	6	3	2
5	1	1	1	1	1	1	1	2	1	1
6	1	1	1	1	1	1	1	1	1	1
7	1	1	2	1	1	1	1	1	1	1
8	2	4	5	3	1	1	1	1	2	1
9	1	3	3	2	1	1	1	2	3	2
10	1	1	2	1	1	1	1	1	2	1

function z produced a vector field that pointed in the direction of the greatest rate of increase in that scalar field. Accordingly, it served as a good model for the *reverse* direction of the general migratory patterns of *G. species*, given the model's initial assumptions regarding density-dependent dispersal. However, by switching the sign of the traditional gradient operator, the vector field opposite of the gradient was rendered:

$$\begin{aligned}\nabla z(x,y) = \Big\langle & \frac{\partial}{\partial x}(6.868 - 9.530y + 3.597y^2 \\ & - 0.526y^3 + 0.026y^4 - 13.478x), \\ & \frac{\partial z}{\partial y}(6.868 - 9.530y + 3.597y^2 \\ & - 0.526y^3 + 0.026y^4 - 13.478x)\Big\rangle \\ = \langle & -13.478\hat{i}, -9.530 + 7.194y \\ & - 1.578y^2 + 0.104y^3\hat{j}\ldots = \vec{z}\end{aligned}$$

Table 2. The data from 'Table 1' were converted into a 3-variable t-chart (where z is a function of x and y, and z represents population at a given set of coordinates) and entered into the ZunZun.com "3-D Function Finder" interface, in accordance with its required data entry format.

X	Y	Z(Pop)	X	Y	Z(Pop)	X	Y	Z(Pop)	X	Y	Z(Pop)	X	Y	Z(Pop)
1	1	1	3	1	1	5	1	1	7	1	1	9	1	1
1	2	1	3	2	1	5	2	1	7	2	1	9	2	3
1	3	1	3	3	1	5	3	1	7	3	2	9	3	3
1	4	1	3	4	1	5	4	1	7	4	1	9	4	2
1	5	1	3	5	1	5	5	1	7	5	1	9	5	1
1	6	2	3	6	4	5	6	1	7	6	1	9	6	1
1	7	5	3	7	6	5	7	1	7	7	1	9	7	1
1	8	8	3	8	9	5	8	2	7	8	1	9	8	2
1	9	7	3	9	7	5	9	1	7	9	1	9	9	3
1	10	6	3	10	4	5	10	1	7	10	1	9	10	2
2	1	1	4	1	1	6	1	1	8	1	2	10	1	1
2	2	1	4	2	1	6	2	1	8	2	4	10	2	1
2	3	1	4	3	1	6	3	1	8	3	5	10	3	2
2	4	1	4	4	1	6	4	1	8	4	3	10	4	1
2	5	1	4	5	1	6	5	1	8	5	1	10	5	1
2	6	3	4	6	2	6	6	1	8	6	1	10	6	1
2	7	7	4	7	3	6	7	1	8	7	1	10	7	1
2	8	10	4	8	6	6	8	1	8	8	1	10	8	1
2	9	9	4	9	3	6	9	1	8	9	2	10	9	2
2	10	5	4	10	2	6	10	1	8	10	1	10	10	1

. . . and taking the reverse:

$$- \vec{z}(x,y) = \langle 13.478\hat{\imath}, 9.530 - 7.194y + 1.578y^2 - 0.104y^3\hat{j} \rangle$$

. . . producing a field whose vectors pointed in the direction of the rate of greatest rate of population density *decrease*. This change in sign resulted in a function that modeled the direction and magnitude of a habitat's population's likely migration at any instant toward a more sink-like habitat, in accordance with the model's initial assumptions.

Next, the vector field ($-\vec{z}$), representing population migration, was subjected to the divergence operator. The divergence of a vector field measures a vector field's source or sink at a given point, returning a value that is positive if there is a net outward flux at a given point (a source) or a value that is negative if there is a net inward flux at a given point (a sink). In this way, the source or sink behavior of any coordinate on the island could be quantitatively measured with a positive or negative value, returned by the function:

$$\nabla \cdot - \vec{z}(x,y) \left\langle \frac{\partial}{\partial x}(13.478) + \frac{\partial}{\partial y}(9.530 - 7.194y + 1.578y^2 - 0.104y^3) \right\rangle$$
$$= \ldots = 0 + 0 - 7.194 + 3.156y - 0.312y^2 \ldots$$

. . . the final sum being either positive (indicating a source) or negative (indicating a sink). Obviously, the above demonstrations use an abridged version of the final population function, for illustrative purposes (with the real equation containing 25 coefficients taken to many decimal places—see Table 3). For models of the actual reverse-gradient and divergence of the complete population function, see Results.

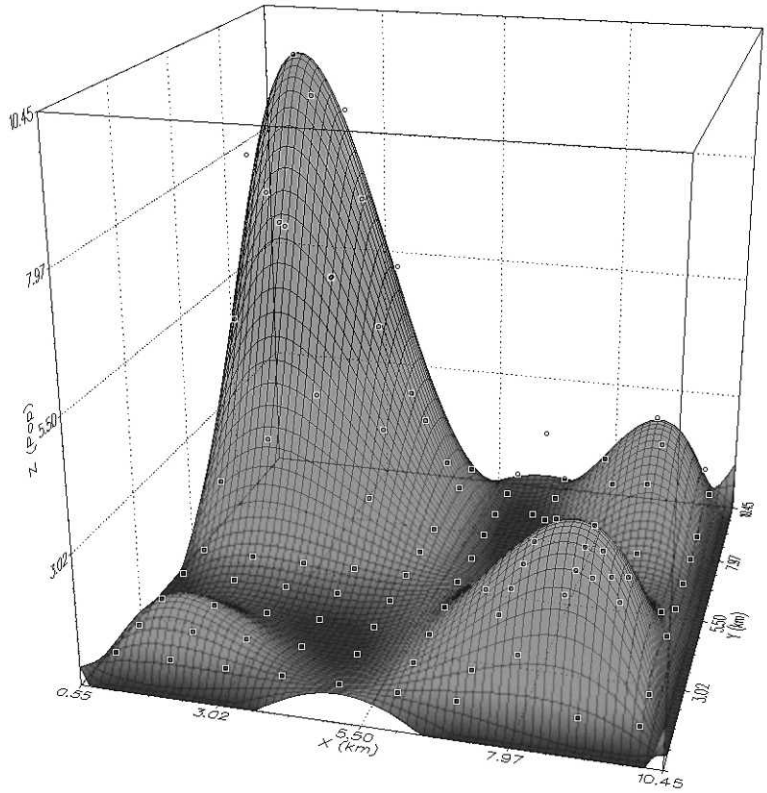

Figure 1. A 3-D function fitted to the *G. species* occurrence data was found using the sum of squared absolute error regression analysis on the ZunZun.com "3-D Function Finder". This permitted the occurrence data to be treated as a scalar field, thus becoming differentiable to traditional vector calculus operators. Here the function z is depicted as a surface in three dimensions.

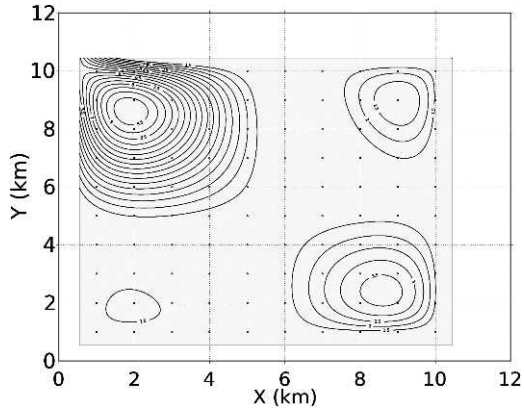

Figure 2. The function z from Figure 1 is depicted as a contour map.

Results

The function of best fit selected to interpolate the population density of *G. species* at any given point is depicted below with an R^2 value of 0.938 and a sum of squared absolute error of 2.6645376234104656E+01:

$$\begin{aligned} z(x,y) = {} & a + by + cy^2 + dy^3 + fy^4 + gx \\ & + hxy + ixy^2 + jxy^3 + kxy^4 \\ & + mx^2 + nx^2y + ox^2y^2 + px^2y^3 \\ & + qx^2y^4 + rx^3 + sx^3y + tx^3y^2 \\ & + ux^3y^3 + vx^3y^4 + wx^4 + Xx^4y \\ & + Yx^4y^2 + Zx^4y^3 + Ax^4y^4 \end{aligned}$$

The coefficients of the function z are shown in Table 3 and the function is modeled below as a surface in Figure 1.

Table 3. The coefficients corresponding to function

$$z(x,y) = a + by + cy^2 + dy^3 + fy^4 + gx + hxy + ixy^2 + jxy^3 + kxy^4 + mx^2 + nx^2y + ox^2y^2 + px^2y^3 + qx^2y^4 + r + sx^3y + tx^3y^2 + ux^3y^3 + vx^3y^4 + wx^4 + Xx^4y + Yx^4y^2 + Zx^4y^3 + Ax^4y^4 :$$

a = 6.8680554786785581E+00
b = -9.5303515613004084E+00
c = 3.5972343591667948E+00
d = -5.2459693070153934E-01
f = 2.5847416473267770E-02
g = -1.3477871639874261E+01
h = 2.1686192762916296E+01
i = -8.8354340017528230E+00
j = 1.3648462954534675E+00
k = -6.8299007871312434E-02
m = 5.6796935692827075E+00
n = -9.0754244005977132E+00
o = 3.6392713824395599E+00
p = -5.5186597628775114E-01
q = 2.7173229232041102E-02
r = -8.4154849774242890E-01
s = 1.3386461779351149E+00
t = -5.2621329110990378E-01
u = 7.8113453658336246E-02
v = -3.7833932610513710E-03
w = 4.0027680646895838E-02
X = -6.3557254221714071E-02
Y = 2.4605357127538363E-02
Z = -3.5923126504040503E-03
A = 1.7177303562831980E-04

After the gradient operator was performed on the population function z and the resulting vector field was reversed (by taking the opposite of the gradient), the general migratory trend for a population at any given point on the island could be shown quantitatively. A model of this migratory vector field using the complete function is shown in Figure 3.

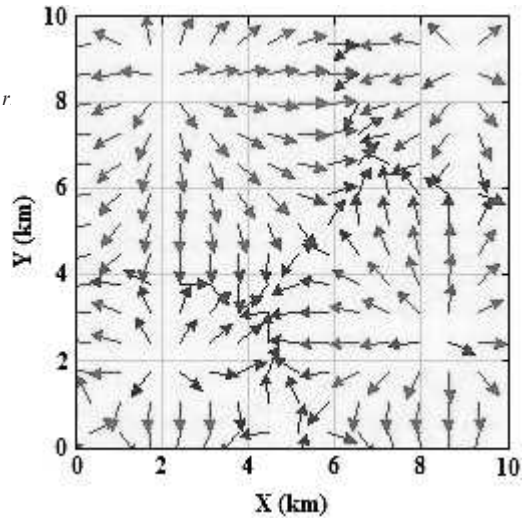

Figure 3. When the reverse-gradient is applied to the population function z ($-\nabla z$), a vector field is returned which approximates the fictional *G. species* migration tendencies assuming density-dependent dispersion.

Discussion

The utility of the modeling technique described above lay in its ability to transform the set of population data into a scalar field which could be represented as a surface in three dimensions. As a scalar field, traditional vector calculus operators, such as the gradient, could be performed on the population function z. However, simply applying the gradient operator on the population function as it stood would have produced a vector field in which each vector pointed in the direction of the greatest increase in z, or increasing population density. Because of the initial assumptions regarding density-dependant dispersal, it was more useful to examine the rate of greatest decrease in population density, precisely the opposite. For this reason, the gradient was simply reversed, thereby producing a vector field whose vectors pointed in the direction of greatest decrease in population density, or, the general migratory trend for any individual of *G. species* at any given point on the island, assuming it conformed to the initial assumptions regarding density-dependent dispersal. A model of this

migratory vector field using the complete function is shown in Figure 3.

Finally, to find the degree to which a point in the field behaves as a source or a sink, one has only to substitute coordinates (or, in this case, km marks) for x and y into the divergence of the reversed population function ($\nabla \cdot -\vec{z}$).

The broad application of this model would be to predict, model, and visualize the likely migratory patterns of any organism in a patchy habitat or metapopulation that conforms to density-dependant dispersal (Fonseca and Hart, 1996; Veit and Lewis, 1996; and Aars and Ims, 2000) and whose most favorable, productive habitats exhibit the most source-like behavior. Additionally, the extent to which any coordinate on a map behaves as a source or a sink could be modeled quantitatively as a signed scalar representing its relative flux. Obviously, this method would not be expected to apply to all real-world situations, but only to those populations which met the assumptions of the Introduction (see Fonseca and Hart, 1996; Veit and Lewis, 1996; and Aars and Ims, 2000). Other taxa for which the model would be reasonably expected to apply are (1) species that generate propagules (spores, seeds, or larvae) and experience no significant directionality due to air currents, etc.; and (2) vagile animals that dislike crowding.

Acknowledgements: I wish to acknowledge the assistance and encouragement of Drs. Brent Hendrixson, Debora Mann, and Sarah Lea Anglin, all of the Millsaps College Biology Department, as well as Dr. Shadow Robinson and Ms. Tracy Sullivan of the Millsaps College Physics and Math Departments, respectively. All models were created using the MatPlotLib plotting library for Python, freely hosted on ZunZun.com.

References

Aars, J., and Ims, R. A. (2000). Population dynamic and genetic consequences of spatial density-dependent dispersal in patchy populations. The American Naturalist, 155, 252–265.

Amarasekare, P. (2004). The role of density-dependent dispersal in source-sink dynamics. Journal of Theoretical Biology. 226, 159–168.

Christopolous, A., and Lew, M. J. (2000). Beyond eyeballing: fitting models to experimental data. Critical Reviews in Biochemistry and Molecular Biology. 35, 359–391.

Fonseca, D. M., and Hart, D. D. (1996). Density-dependent dispersal of black fly neonates is mediated by flow. Oikos. 75, 49–58.

Hanski, I. (1991). Metapopulation dynamics: brief history and conceptual domain. Biological Journal of the Linnean Society. 42, 3–16.

Johnson, D. M. (2004). Source-sink dynamics in a temporally heterogeneous environment. Ecology. 85(7), 2037–2045.

Lancaster, P., and Salkauskas, K. (1986). Curve and surface fitting: an introduction. London: Academic Press.

Levins, R. (1969). Some demographic and genetic consequences of environmental heterogeneity for biological control. Bulletin of the Entomological Society of America. 15, 237–240.

Pulliam, H. R. (1988). Sources, sinks, and population regulation. The American Naturalist. 132, 652–661.

Van Horne, B. (1983). Density as a misleading indicator of habitat quality. The Journal of Wildlife Management. 47, 893–901.

Veit, R. R. and Lewis, M. A. (1996). Dispersal, population growth, and the Allee effect: dynamics of the house finch invasion of eastern North America. The American Naturalist. 148, 255–274.

Received 10 June 2011; accepted 30 November 2011.